

## Investigation of *N*-Aryl-3-alkylidenepyrrolinones as Potential Niemann–Pick Type C Disease Therapeutics

Casey C. Cosner,<sup>†</sup> John T. Markiewicz,<sup>†</sup> Pauline Bourbon,<sup>†</sup> Christopher J. Mariani,<sup>†</sup> Olaf Wiest,<sup>†</sup> Madalina Rujoi,<sup>‡</sup> Anton I. Rosenbaum,<sup>‡</sup> Amy Y. Huang,<sup>‡</sup> Frederick R. Maxfield,<sup>‡</sup> and Paul Helquist<sup>\*,†</sup>

<sup>†</sup>Department of Chemistry and Biochemistry, University of Notre Dame, 250 Nieuwland Science Hall, Notre Dame, Indiana 46556, and  
<sup>‡</sup>Department of Biochemistry, Weill Medical College of Cornell University, 1300 York Avenue, New York, New York 10065

Received May 25, 2009

A five-step synthesis of an array of *N*-aryl-3-alkylidenepyrrolinones, which are potential Niemann–Pick type C (NPC) disease therapeutics, is described. The synthetic route allows for the production of analogues, including photoaffinity and biotinylated derivatives. Compound **1a** increased esterification by acyl-coenzyme A:cholesteryl acyltransferase in NPC1 mutant cells. It also decreased LDL uptake and increased cholesterol efflux in both NPC1-deficient and normal cells.

### Introduction

Niemann–Pick type C disease (NPC<sup>C</sup>)<sup>1</sup> is a rare autosomal recessive lipid storage disorder with most commonly a fatal neurodegenerative course.<sup>2</sup> The disease mainly affects children, but juvenile and adult forms of the disease are also known. Some of the clinical symptoms of this disease include liver abnormalities, learning difficulties, epilepsy, vertical gaze palsy, seizures, neonatal jaundice, and finally neurodegeneration, which is the most common cause of death.<sup>1a</sup> On the cellular level, the most pronounced observation is an abnormal accumulation of lipids such as cholesterol, glycosphingolipids, and some phospholipids in late endosome/lysosome (LE/LY)-like storage organelles (LSOs).<sup>3</sup>

NPC disease is caused by mutations in one of two genes, *npc1* (95% of all cases) and *npc2*.<sup>4</sup> The *npc1* gene encodes the 1278-residue integral membrane NPC1 protein,<sup>5</sup> which contains 13 putative transmembrane domains. The *npc2* gene encodes the soluble protein NPC2 found in endosomes and possesses a cholesterol binding site.<sup>6</sup> It has recently been reported that while both NPC1 and NPC2 proteins bind cholesterol, NPC2 accelerates the transfer of cholesterol from NPC1 to liposomes, indicating a potential necessary function of the two proteins.<sup>7</sup> There is currently no cure for NPC disease. While attempts have been made to develop effective treatment options,<sup>1d,8</sup> there remains a significant need to discover and develop useful therapeutics to treat this disease.

In 2006, the Maxfield laboratory reported an automated filipin-based high-throughput screening procedure that measures the levels of filipin-bound cholesterol in the LSOs and also overall in the cell, based on images of cells stained with filipin, a fluorescent antibiotic.<sup>9</sup> By using this new technique,

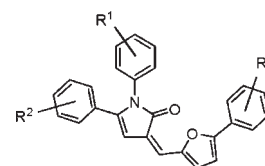


**Figure 1.** Pyrrolinones of general structure **1**.

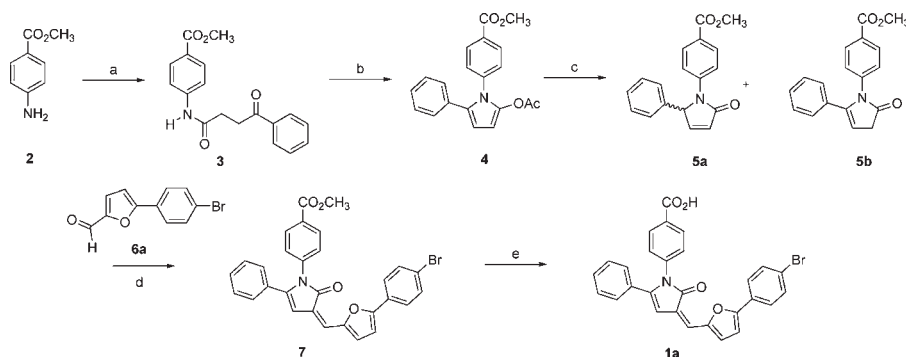
the Maxfield laboratory was able to screen an initial library of 14956 compounds and found that several of these compounds lowered the filipin fluorescence intensity in the lysosomal storage compartments of CT60 and CT43 NPC1 mutant Chinese hamster ovary (CHO) cells. This finding indicated that the free cholesterol content of these organelles was reduced.

Of the initial set of 14956 compounds, several pyrrolinones of general structure **1** (Figure 1) exhibited significantly above average activity and consistent dose response. In addition to this activity, some of these compounds showed only mild toxicity toward normal cells in contrast to many of the other hit compounds. The dual observation of cholesterol reduction and mild toxicity of this pyrrolinone family made them an attractive target for further investigation as potential therapeutic leads for NPC disease. As such, we sought to develop a general synthesis that would allow the efficient production of a series of analogues for assay of activity in NPC1-deficient cells.

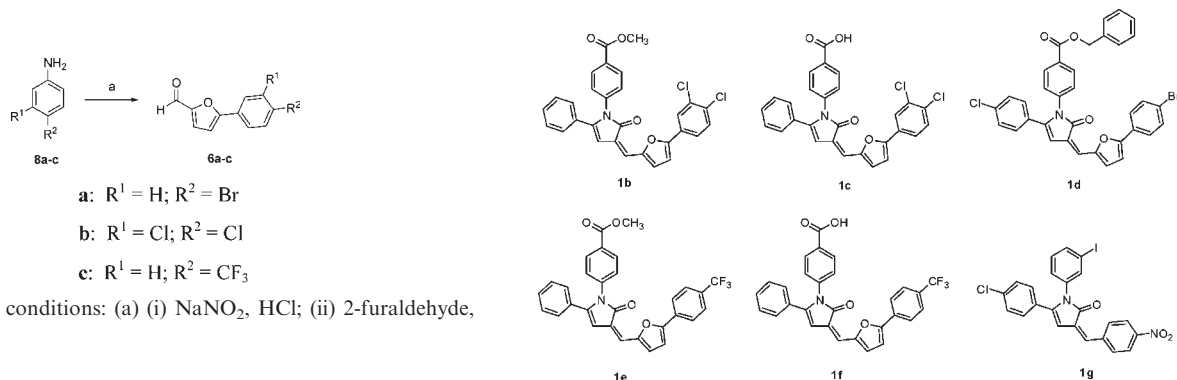
The original source of **1** for screening was a commercially obtained library for which the details of synthesis were not available and from which only very limited quantities of **1** of questionable purity could be obtained. Therefore, the initial goal of the work reported in this paper was to develop an efficient, flexible, high-throughput pathway to the desired pyrrolinones with a variety of substitution patterns with both good quantity and purity. In addition to providing a series of analogues, a synthesis of pure compounds would minimize the risk of false positives in further assays. A survey of the literature revealed that there have been previous reports of the synthesis of the core 3-alkylidene-4-pyrrolin-2-one scaffold.<sup>10</sup> Many of these routes utilize 3-alkylidene-furan-2-ones as starting materials.<sup>10a,10b11</sup> We found that these protocols were not amenable to our needs. Given the deficiencies in

\*To whom correspondence should be addressed. Phone: (574)-631-7822. Fax: (574)-631-6652. E-mail: phelquis@nd.edu.

<sup>†</sup>Abbreviations: ACAT, acyl-coenzyme A:cholesteryl acyltransferase; CHO cells, Chinese hamster ovary cells; DiI, 1,1'-dioctadecyl-3,3,3',3'-tetramethylindocarbocyanine perchlorate; DMAP, 4-dimethylamino pyridine; EDC, *N*-(3-dimethylaminopropyl)-*N'*-ethylcarbodiimide hydrochloride; GC, gas chromatography; LDL, low-density lipoprotein; LE/LY, late endosomes/lysosomes; LSO, LE/LY-like organelles; NPC, Niemann–Pick type C disease; TMSN<sub>3</sub>, trimethylsilyl azide.

Scheme 1<sup>a</sup>

<sup>a</sup> Reagents and conditions: (a) 3-benzoylpropionic acid, EDC, DMAP, CH<sub>2</sub>Cl<sub>2</sub>, 0 °C, 80%; (b) AcCl, DMAP, reflux, 90%; (c) NaBH<sub>4</sub>, MeOH, 0 °C, 85%; (d) **6a**, NaOAc, Ac<sub>2</sub>O, 100 °C, 75%; (e) LiI, pyridine, reflux, 95%.

Scheme 2<sup>a</sup>

<sup>a</sup> Reagents and conditions: (a) (i) NaNO<sub>2</sub>, HCl; (ii) 2-furaldehyde, CuCl<sub>2</sub>, acetone.

previous syntheses, we set out to establish our own synthetic pathway toward the production of **1**.

## Chemistry

Our general route is illustrated by the synthesis of **1a** (Scheme 1). Coupling methyl *p*-aminobenzoate **2** to benzoylpropionic acid using 1-ethyl-3-(3-dimethylaminopropyl) carbodiimide hydrochloride (EDC) and catalytic 4-dimethylaminopyridine (DMAP) afforded ketoamide **3**. Ketoamide **3** was cyclized to acetoxy pyrrolone **4** after refluxing in acetyl chloride.<sup>12</sup> The acetyl group was cleaved using sodium borohydride in methanol, providing an inconsequential mixture of **5a** and **5b** in approximately a 95:5 ratio. The use of strong hydrolyzing agents such as hydroxide in this step led to decomposition of the substrates and ring-opened products.

We next prepared **6a** (Scheme 2) by diazotization of 4-bromoaniline (**8a**), followed by a copper-promoted reaction with furfural.<sup>13</sup> The penultimate aldol step involved submitting the mixture of **5a** and **5b** with **6a** to Perkin condensation conditions. The *Z*-olefin **7** was the only observed product as determined by NOESY NMR studies. The final deprotection step using lithium iodide in refluxing pyridine afforded the free acid **1a**.<sup>14</sup> Using this pathway, we have produced up to 5 g of **1a** in highly pure form compared to the mg quantities of less pure material obtained from the commercial library.

To demonstrate the flexibility of our pathway and to obtain a series of analogues for NPC assays, we applied our route to the syntheses of **1b–g** (Figure 2). To obtain these analogues, the individual components were modified. The methyl ester **2** was replaced with a benzyl ester, the starting benzoylpropionic acid was derivatized to include a chlorine, and the 5-arylfurfural **6a** was replaced by aldehydes **6b** and **6c** as well as by *p*-nitrobenzaldehyde.

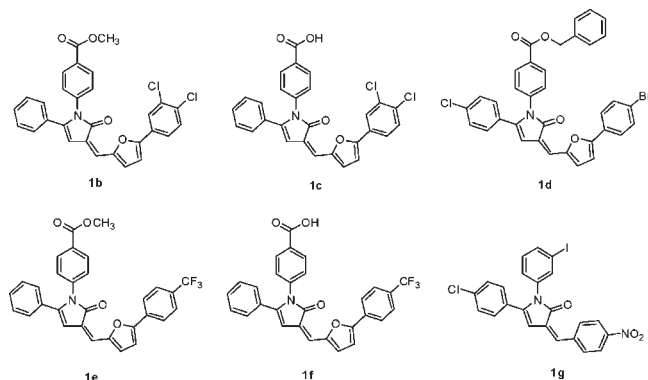


**Figure 2.** Library of pyrrolinone analogues produced by the general scheme.

In addition to the study of analogues, another strategy to develop improved therapeutic agents is to identify their biological targets. With this information in hand, the mechanisms of action can be probed and a combination of experimental and computational methods can be employed to design the improved compounds. We therefore set out to obtain a derivative of **1a** for photoaffinity labeling studies to identify its biological target.<sup>15</sup> Of the many classes of photoaffinity labeling agents available, the azides are particularly appealing for the case of **1a** in that the bromide substituent should be suitable for nucleophilic exchange to produce the azide derivative **10**.

The synthesis of **10** (Scheme 3) commenced with an attempted copper-catalyzed aromatic substitution known to produce azides from the corresponding bromides.<sup>16</sup> We found that the azide was presumably produced but was quickly converted to the amine **9** before consumption of the starting material was completed. This reaction was driven fully to the amine by the use of a stoichiometric equivalent of cuprous iodide. Amine **9** was converted to azide **10** using Moses' mild diazo transfer reaction.<sup>17</sup>

Alternatively, we also sought to obtain a derivative for biological target identification by using a biotin label<sup>18</sup> in the form of **11**. The synthesis of this labeled compound began by coupling known aminoazide **12**<sup>19</sup> to **1a** using EDC to produce **13** (Scheme 4). The completion of the synthesis of the labeled compound was based on using the biotin propargylamide **15**.<sup>20</sup> This compound was prepared from the readily available biotin-NHS ester **14** and propargyl amine.<sup>21</sup> With both units in hand, a copper-catalyzed cyclization<sup>22</sup> between the azide **13** and terminal alkyne **15** resulted in the final biotinylated

analogue **17**. The use of both the biotinylated analogue **11** and the azide **10** will be the subjects of a separate investigation of cellular targets.

### Biological Activity

The effects of pyrrolinones **1a–g** on cholesterol levels in the LSOs in CT60 and CT43 NPC1 mutant CHO cells had been previously assayed using a filipin-based microscopy method.<sup>9</sup> Of these compounds, only **1a** (labeled as 1a13 in the previous publication)<sup>9</sup> exhibited significant reduction of cholesterol accumulated in the lysosomal storage organelles. Using a filipin-based image analysis assay that quantifies cholesterol accumulation in the LSOs (see details in ref 9 for the assay called LSO compartment ratio assay), it had been shown that **1a** caused an 80% decrease in fluorescence in CT43 cells and 30% in CT60 cells, at a concentration of 10  $\mu\text{M}$ .<sup>9</sup> The analogues **1b–1g** showed no corresponding activity. Therefore, **1a** was selected for more thorough study.

In particular, the effects of **1a** on cholesterol metabolism and transport in CT60 NPC1-defective CHO cells were investigated. In cells with normal sterol trafficking, cholesterol (mostly esterified) is internalized into cells via lipoproteins and delivered to LE/LY, where hydrolysis of cholesteryl esters by lysosomal acid lipase takes place.<sup>23</sup> Free cholesterol is then exported from the LE/LY and delivered to the plasma membrane and extracellular acceptors, as well as the endoplasmic reticulum, where cholesterol is esterified by the acyl-coenzyme A:cholesterol acyltransferase (ACAT) and deposited as lipid droplets.<sup>24</sup> Cholesterol esters formed by ACAT are then hydrolyzed by cytoplasmic neutral cholesterol ester hydrolases. While low-density lipoprotein (LDL) uptake and its

delivery to LE/LY are all normal in NPC-deficient cells, the rate of cholesterol efflux from the LE/LY is severely reduced.<sup>25</sup> As a consequence, there is an obstruction in cholesterol trafficking and hence a significant decrease in the homeostatic responses in NPC-deficient cells.

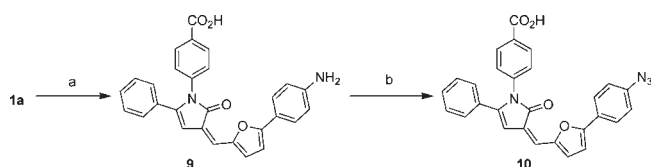
We investigated the effect of **1a** on cholesterol efflux and on the uptake of LDL-derived cholesterol in NPC1-deficient cells. We also evaluated the overall levels of cholesteryl ester in the cell and the esterification promoted by ACAT in the presence of this compound. Experimental results, discussed below, are summarized in Figure 3 and Table 1.

We measured the effect of compound **1a** on cholesterol efflux to extracellular acceptors in the serum (e.g., high density lipoproteins) in the following cell lines: NPC1-deficient cell line CT60, its non-NPC1 parental line 25RA, and the non-NPC1 cell line TRVb1. 25RA cells are CHO cells with a gain of function mutation in the sterol regulatory element-binding protein cleavage activating protein (SCAP) gene. TRVb1 cells are apparently normal CHO cells transfected with a human transferrin receptor.<sup>27</sup> The major cholesterol efflux from the CHO cells would be mediated by ATP-binding cassette transporter.<sup>28</sup> Changes in the efflux in the presence of **1a** were compared to solvent-treated control cells. We observed (Figure 3) that compound **1a** increased efflux not only in NPC1-deficient CT60 cells but also in the 25RA and TRVb1 cells, which have normal NPC1.

We studied the direct effect of **1a** on LDL endocytosis by incubating the cells for a short time (35 min) with **1a** and DiI-labeled LDL. We also tested the longer term effect of **1a** on LDL uptake by incubating the cells for 18 h with **1a** and DiI-LDL. We observed that both in NPC1-deficient CT60 cells as well as the NPC wild type 25RA parental cells **1a** causes a significant inhibition of LDL internalization (DiI-LDL uptake) during long (18 h) treatments. However, no significant changes in DiI-LDL uptake during short (35 min) incubations were observed, indicating that there is not a direct effect on LDL binding.

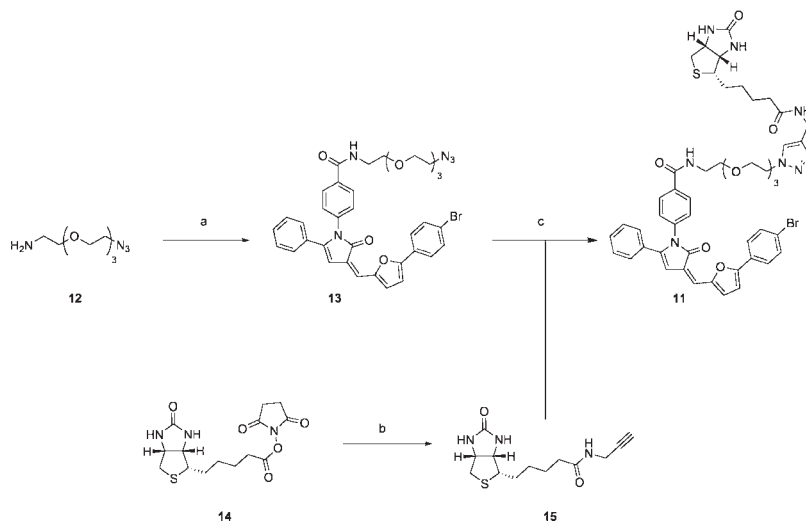
When we measured the overall cellular content of cholesteryl esters by gas chromatography (GC), we found no significant change in the overall cholesteryl ester levels (Table 1). However, when we tested the effect of **1a** on cholesterol esterification by ACAT by quantifying the incorporation of [<sup>14</sup>C]-oleic acid into cholesteryl-[<sup>14</sup>C]-oleate, we

### Scheme 3<sup>a</sup>



<sup>a</sup> Reagents and conditions: (a)  $\text{Na}_2\text{CO}_3$ ,  $\text{NaN}_3$ ,  $\text{CuI}$ , *N,N'*-dimethylethylenediamine, DMSO, 85%; (b) *t*BuONO,  $\text{TMSN}_3$ , DMSO, 74%.

### Scheme 4<sup>a</sup>



<sup>a</sup> Reagents and conditions: (a) **1a**, EDC, DMAP, pyridine, 65%; (b) propargylamine, DMF, 92%; (c) **15**,  $\text{CuSO}_4$ , sodium ascorbate, acetone, 73%.

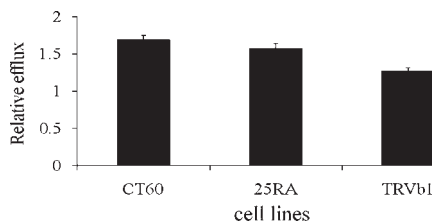


**Figure 3.** Relative increase in cholesterol efflux by **1a** in normal (TRVb1, 25RA) and mutant (CT60) CHO cells. Cells were labeled with  $1 \mu\text{Ci/ml}$  [ $^3\text{H}$ ]-cholesterol for 24 h and then incubated for 18 h with  $10 \mu\text{M}$  **1a**. Efflux was expressed as the radioactivity of the supernatant relative to the total of the radioactivity in the supernatant and the cell monolayer. For solvent-treated (control) cells, the mean values of supernatant/total were:  $0.069 \pm 0.003$  for CT60 cells,  $0.066 \pm 0.004$  for 25RA cells, and  $0.214 \pm 0.006$  for TRVb1 cells. Experimental data of **1a**-treated cells are presented as relative efflux with respect to the control ( $p < 0.001$ ). Five independent experiments ( $n = 25$ ) were run in CT60 cells, and two independent experiments ( $n = 10$ ) for 25RA and TRVb1 cells.

**Table 1.** Summary of the Effects of  $10 \mu\text{M}$  **1a** in NPC1-Deficient CT60 Cells<sup>a</sup>

| assay   | average value $\pm$ SE (fraction of the control) |
|---|--|
| endocytosis of DiI-LDL by CT60 cells in 35 min  | $0.93 \pm 0.05$                                  |
| endocytosis of DiI-LDL by 25RA cells in 35 min  | $1.16 \pm 0.31$                                  |
| endocytosis of DiI-LDL by CT60 cells in 18 h  | $0.59 \pm 0.06^{*b}$                             |
| endocytosis of DiI-LDL by 25RA cells in 18 h  | $0.67 \pm 0.03^{*b}$                             |
| ACAT esterification: Incorporation of [ $^{14}\text{C}$ ]-oleic acid cholesteryl esters | $1.49 \pm 0.13^{*b}$<br>$1.05 \pm 0.10$          |

<sup>a</sup> The effect of **1a** on LDL internalization was evaluated by quantifying the fluorescence intensity of DiI per  $\mu\text{g}$  cell protein, normalized to the mean value of solvent-treated samples. The impact of **1a** on esterification by ACAT was estimated by quantifying the incorporation of [ $^{14}\text{C}$ ]-oleic acid into esters per cellular protein content. For solvent-treated cells the mean value was  $(14 \pm 1)$  pmol cholesteryl-[ $^{14}\text{C}$ ] ester/ $\mu\text{g}$  cell protein.<sup>26</sup> The effect of **1a** on overall cholesteryl ester levels in the cell was determined by GC. The mean value for solvent-treated cells was  $(0.042 \pm 0.004)$   $\mu\text{g}$  cholesteryl ester/ $\mu\text{g}$  cell protein.<sup>26</sup> <sup>b</sup> indicates  $p < 0.02$ .

observed an increase in ACAT esterification upon treatment of CT60 cells with **1a** for 18 h. For the solvent-treated CT60 cells, the average experimental value corresponding to ACAT esterification is  $(14 \pm 1)$  pmol cholesteryl-[ $^{14}\text{C}$ ]-oleate/ $\mu\text{g}$  cellular protein,<sup>9</sup> while for **1a**-treated CT60 cells, the value is about  $20.9$  pmol/ $\mu\text{g}$  protein. The restoration by **1a** of the ACAT esterification in NPC-deficient CT60 cells is significant, because in the solvent-treated non-NPC mutant 25RA, the experimental value is  $37 \pm 3$  pmol cholesteryl-[ $^{14}\text{C}$ ]-oleate/ $\mu\text{g}$  cellular ( $n = 27$ , six independent experiments).

In this paper and in our previous study,<sup>9</sup> we described several effects of **1a** on NPC1-deficient cells. There is reduced filipin labeling of unesterified cholesterol in the LSOs,<sup>9</sup> and there is an increase in efflux of cholesterol to extracellular acceptors (Figure 3), decreased uptake of LDL (Table 1), and increased cholesterol esterification by ACAT (Table 1). All of these changes would be consistent with release of cholesterol from the LSOs in response to treatment with **1a**. The cholesterol released from the LSOs would be a substrate for ACAT and would be expected to increase incorporation of radiolabeled oleate into cholesteryl ester droplets. This released cholesterol would also be expected to increase cholesterol efflux and to down-regulate the expression of LDL receptors through the SREBP pathway.<sup>30</sup> The lack of an increase in

cellular cholesteryl esters (Table 1) may seem paradoxical because there is increased esterification by ACAT. However, it has been reported that net hydrolysis of lipoprotein-derived cholesteryl esters in lysosomes stalls when levels of unesterified cholesterol in these organelles becomes high, as would be the case in NPC1-deficient cells.<sup>29</sup> The amounts of cholesteryl esters in the LSOs of untreated NPC1-deficient cells is not known, but loss of this cholesteryl ester pool may balance the increase in the cytoplasmic lipid droplets. We also found that total unesterified cellular cholesterol as measured by GC was increased in the cells treated with **1a**, and total filipin fluorescence from the whole cell area was essentially unchanged.<sup>9</sup> Although NPC1-deficient cells have high amounts of cholesterol in the LSOs, their other membranes may actually be cholesterol-poor as compared to wild type cells.<sup>1</sup> Thus, a treatment that releases cholesterol from the LSOs would not be expected to decrease the overall cholesterol level in the cells. The previously reported increase in cholesterol in response to **1a** is not fully understood. It may reflect a transient condition as the cells deal with release of a large amount of cholesterol from the LSOs.

Because compound **1a** increased not only the esterification by ACAT but also cholesterol efflux to extracellular acceptors, this compound could be considered a valuable candidate for directly promoting sterol efflux from the LE/LY in NPC1-deficient and other cells.

## Conclusion

In summary, we have devised a concise and efficient route for the production of the goal *N*-aryl-3-alkylidene-pyrrolinones comprising five simple steps. When applied to initial compound **1a**, the route provided the desired product in 43% overall yield. The route has also facilitated the synthesis of analogues. Furthermore, using our primary scaffold, we were able to synthesize photoaffinity labeled and biotinylated derivatives for use in separate investigations. Studies of **1a** show that it decreases the LDL uptake and increases ACAT esterification in mutant-NPC1 cells and it increases cholesterol efflux in NPC1 mutant and normal cells.

## Experimental Section

All experiments were run under inert atmosphere unless otherwise stated. Thin layer chromatography (TLC) was conducted using precoated silica gel 60 F<sub>254</sub> plates from EMD Chemicals. Infrared spectra were recorded on a Perkin-Elmer Paragon 1000 FT-IR spectrometer. HRMS data were recorded on a JEOL JMS-AX505HA double sector mass spectrometer using FAB. NMR spectra were recorded using Varian-INOVA 500 and 300 spectrometers operating at 500 MHz ( $^1\text{H}$ ) and 125 MHz ( $^{13}\text{C}$ ) and 300 MHz ( $^1\text{H}$ ) and 75 MHz ( $^{13}\text{C}$ ), respectively. Chemical shifts are given in ppm relative to residual solvent peaks:  $^1\text{H}$  (7.27 for  $\text{CDCl}_3$  and 2.5 for  $\text{DMSO}-d_6$ ) and  $^{13}\text{C}$  (77.23 for  $\text{CDCl}_3$  and 39.51 for  $\text{DMSO}-d_6$ ). Flash chromatography was performed using EcoChrome 60 Å silica gel. All tested compounds were  $> 95\%$  pure by HPLC.

(*Z*)-4-(3-((5-(4-Bromophenyl)furan-2-yl)methylene)-2-oxo-5-phenyl-2,3-dihydro-1*H*-pyrrol-1-yl)benzoic Acid (**1a**). Pyrrolinone **7** (1.15 g, 1.9 mmol) was added to freshly distilled pyridine (8 mL) at 23 °C. To this mixture was added anhydrous lithium iodide (3.56 g, 26.6 mmol). This mixture was heated to reflux and stirred at this temperature for 14 h. During this time, the mixture became homogeneous and darkened in color. The reaction mixture was cooled to 23 °C and poured into ice cold 1 N HCl. The pH of the solution was adjusted to 2, and the

precipitated red solid was collected by vacuum filtration. The solid cake was washed with 1 N HCl (2 × 20 mL) and DI water (2 × 20 mL). The solid was allowed to air-dry, affording 1.12 g of **1a** (95%). <sup>1</sup>H NMR matched that of an commercial sample; mp = > 200 °C. <sup>1</sup>H NMR (500 MHz, DMSO-*d*<sub>6</sub>) δ 7.92 (d, *J* = 8 Hz, 2H), 7.83 (d, *J* = 8 Hz, 2H), 7.71 (d, *J* = 8 Hz), 7.38–7.34 (m, 5H), 7.32–7.29 (m, 2H), 7.23–7.20 (m, 3H), 6.84 (s, 1H). <sup>13</sup>C (125 MHz, DMSO-*d*<sub>6</sub>) δ 169.2, 167.4, 156.4, 152.7, 146.7, 140.2, 132.9, 131.0, 130.4, 129.9, 129.5, 129.3, 128.9, 128.3, 127.6, 127.2, 126.9, 125.7, 122.6, 118.1, 111.4, 111.4, 104.5. HRMS (FAB) calcd for C<sub>28</sub>H<sub>18</sub>BrNO<sub>4</sub> (M + H)<sup>+</sup> 512.0497, found 512.0485. IR (KBr pellet): 3418, 3057, 1706, 1683, 1605, 1470, 1173, 1112 cm<sup>-1</sup>.

**Acknowledgment.** We thank the Ara Parseghian Medical Research Foundation and the University of Notre Dame for financial support of this research. This work was also supported by NIH grant R37-DK27083 to F.R.M. Also, we thank Prof. J. David Warren and Dr. Guangtao Zhang of the Milstein Organic Synthesis Core Facility of Cornell University for their help with DiI chromatography and B. Attawut for help in preparing DiI-LDL. M.R. was supported by a grant from the W. M. Keck Foundation.

**Supporting Information Available:** Detailed experimental procedures and characterization data for all intermediates, products, and biochemical assays are available. This material is available free of charge via the Internet at <http://pubs.acs.org>.

## References

- (1) For recent reviews, see: (a) Sturley, S. L.; Patterson, M. C.; Balch, W.; Liscum, L. The pathophysiology and mechanisms of NP-C disease. *Biochim. Biophys. Acta, Mol. Cell Biol. Lipids* **2004**, *1685*, 83–87. (b) Mukherjee, S.; Maxfield, F. R. Lipid and cholesterol trafficking in NPC. *Biochim. Biophys. Acta, Mol. Cell Biol. Lipids* **2004**, *1685*, 28–37. (c) Maxfield, F. R.; Tabas, I. Role of cholesterol and lipid organization in disease. *Nature* **2005**, *438*, 612–621. (d) Wraith, J. E.; Imrie, J. Understanding Niemann–Pick Disease Type C and Its Potential Treatment. Blackwell Publishing Co.: Malden, MA, 2007; pp 1–36.
- (2) Cataldo, A. M.; Nixon, R. A. Neuronal Protein Trafficking in Alzheimer's Disease and Niemann–Pick Type C Disease. In *Protein Trafficking in Neurons*; Bean, A. J., Ed.; Academic Publishing: New York, 2007; pp 391–411.
- (3) Liscum, L.; Ruggiero, R. M.; Faust, J. R. The intracellular transport of low-density lipoprotein derived cholesterol is defective in Niemann–Pick type C fibroblasts. *J. Cell Biol.* **1989**, *108*, 1625–1636.
- (4) Walkley, S. U.; Suzuki, K. Consequences of NPC1 and NPC2 loss of function in mammalian neurons. *Biochim. Biophys. Acta, Mol. Cell Biol. Lipids* **2004**, *1685*, 48–62.
- (5) Infante, R. E.; Abi-Mosleh, L.; Radhakrishnan, A.; Dale, J. D.; Brown, M. S.; Goldstein, J. L. Purified NPC1 Protein: I. Binding of Cholesterol and Oxysterols to a 1278-Amino Acid Membrane Protein. *J. Biol. Chem.* **2008**, *283*, 1052–1063.
- (6) Xu, S.; Benoff, B.; Liou, H. L.; Lobel, P.; Stock, A. M. Structural basis of sterol binding by NPC2, a lysosomal protein deficient in Niemann–Pick type C2 disease. *J. Biol. Chem.* **2007**, *282*, 23525–23531.
- (7) Infante, R. E.; Wang, M. L.; Radhakrishnan, A.; Kwon, H. J.; Brown, M. S.; Goldstein, J. L. NPC2 facilitates bidirectional transfer of cholesterol between NPC1 and lipid bilayers, a step in cholesterol egress from lysosomes. *Proc. Natl. Acad. Sci. U.S.A.* **2008**, *105*, 15287–15292.
- (8) (a) Liscum, L.; Arnio, E.; Anthony, M.; Howley, A.; Sturley, S. L.; Agler, M. Identification of a pharmaceutical compound that partially corrects the Niemann–Pick C phenotype in cultured cells. *J. Lipid Res.* **2002**, *43*, 1708–1717. (b) Patterson, M. C.; Platt, F. Therapy of Niemann–Pick disease, type C. *Biochim. Biophys. Acta, Mol. Cell Biol. Lipids* **2004**, *1685*, 77–82. (c) Helquist, P.; Wiest, O. Current status of drug therapy development for Niemann–Pick type C disease. *Drugs Future* **2009**, *34*, 315–331.
- (9) Pipalia, N. H.; Huang, A.; Ralph, H.; Rujoi, M.; Maxfield, F. R. Automated microscopy screening for compounds that partially revert cholesterol accumulation in Niemann–Pick C cells. *J. Lipid Res.* **2006**, *47*, 284–301.
- (10) (a) Egorova, A. Y.; Sedavkina, V. A.; Timofeeva, Z. Y. Synthesis and structure of 5-alkyl(aryl)pyrrol-2-ones. *Chem. Heterocycl. Compd.* **2001**, *37*, 550–553. (b) Egorova, A. Y. Synthesis of arylidene derivatives of N-unsubstituted pyrrolin-2-ones. *Russ. Chem. Bull., Int. Ed.* **2002**, *51*, 183–184. (c) Egorova, A. Y.; Nesterova, V. V. Synthesis of arylidene derivatives of 1-aryl-3H-pyrrol-2-ones. *Chem. Heterocycl. Compd.* **2004**, *40*, 1002–1006.
- (11) Filler, R.; Piasek, E. J.; Leipold, H. A. α-Benzylidene-γ-phenyl-Δ<sup>β,γ</sup>-butenolide. *Org. Synth.* **1963**, *43*, 3–5.
- (12) Tsolomiti, G.; Tsolomitis, A. An unexpected simple synthesis of N-substituted 2-acetoxy-5-arylpyrroles and their hydrolysis to 3- and 4-pyrrolin-2-ones. *Tetrahedron Lett.* **2004**, *45*, 9353–9355.
- (13) Holla, B. S.; Malini, K. V.; Sarojini, B. K.; Poojary, B. Novel Three-Component Synthesis of Triazinotiazolones. *Synth. Commun.* **2005**, *35*, 333–340.
- (14) (a) Elsinger, F.; Schreiber, J.; Eschenmoser, A. Notiz über die Selektivität der Spaltung von Carbonsäure-methylestern mit Lithiumjodid. *Helv. Chim. Acta* **1960**, *43*, 113–118. (b) Fisher, J. W.; Trinkle, K. L. Iodide Dealkylation of Benzyl, PMB, PNB, and t-Butyl N-acyl Amino Acid Esters via Lithium Ion Coordination. *Tetrahedron Lett.* **1994**, *35*, 2505–2508.
- (15) Fleming, S. A. Chemical Regents in Photoaffinity Labeling. *Tetrahedron* **1995**, *51*, 12479–12520.
- (16) Andersen, J.; Madsen, U.; Björkling, F.; Liang, X. Rapid Synthesis of Aryl Azides from Aryl Halides under Mild Conditions. *Synlett* **2005**, 2209–2213.
- (17) Barral, K.; Moorhouse, A. D.; Moses, J. E. Efficient Conversion of Aromatic Amines into Azides: A One-Pot Synthesis of Triazole Linkages. *Org. Lett.* **2007**, *9*, 1809–1811.
- (18) Marks, K. M.; Nolan, G. P. Chemical labeling strategies for cell biology. *Nat. Methods* **2006**, *3*, 591–596.
- (19) Schwabacher, A. W.; Lane, J. W.; Schiesher, M. W.; Leigh, K. M.; Johnson, C. W. Desymmetrization Reactions: Efficient Preparation of Unsymmetrically Substituted Linker Molecules. *J. Org. Chem.* **1998**, *63*, 1727–1729.
- (20) Zhao, X. Z.; Semenova, E. A.; Liao, C.; Nicklaus, M.; Pommier, Y.; Burke, T. R. Biotinylated biphenyl ketone-containing 2,4-dioxobutanoic acids designed as HIV-1 integrase photoaffinity ligands. *Bioorg. Med. Chem.* **2006**, *14*, 7816–7825.
- (21) Susumu, K.; Uyeda, H. T.; Medintz, I. T.; Pons, T.; Delehanty, J. B.; Mattoussi, H. Enhancing the Stability and Biological Functionalities of Quantum Dots via Compact Multifunctional Ligands. *J. Am. Chem. Soc.* **2007**, *129*, 13987–13996.
- (22) Rostovtsev, V. V.; Green, L. G.; Fokin, V. V.; Sharpless, K. B. A Stepwise Huisgen Cycloaddition Process: Copper(I)-catalyzed Regioselective “Ligation” of Azides and Terminal Alkynes. *Angew. Chem., Int. Ed.* **2002**, *41*, 2596–2599.
- (23) (a) Goldstein, J. L.; Dana, S. E.; Faust, J. R.; Beaudet, A. L.; Brown, M. S. Role of lysosomal acid lipase in the metabolism of plasma low density lipoprotein. Observations in cultured fibroblasts from a patient with cholesteryl ester storage disease. *J. Biol. Chem.* **1975**, *250*, 8487–8495. (b) Goldstein, J. L.; Basu, S. K.; Brown, M. S. Receptor-mediated endocytosis of low-density lipoprotein in cultured cells. *Methods Enzymol.* **1983**, *98*, 241–260.
- (24) Chang, T. Y.; Chang, C. C. Y.; Cheng, D. Acyl-coenzyme A: cholesterol acyltransferase. *Annu. Rev. Biochem.* **1997**, *66*, 613–638.
- (25) Sokol, J.; Blanchette-Mackie, J.; Kruth, H. S.; Dwyer, N. K.; Amende, L. M.; Butler, J. D.; Robinson, E.; Patel, S.; Brady, R. O.; Comly, M. E.; Vanier, M. T.; Pentchev, P. G. Type C Niemann–Pick disease. Lysosomal accumulation and defective intracellular mobilization of low density lipoprotein cholesterol. *J. Biol. Chem.* **1988**, *263*, 3411–3417.
- (26) Rosenbaum, A. I.; Rujoi, M.; Huang, A. Y.; Du, H.; Grabowski, G. A.; Maxfield, F. R. *Biochim. Biophys. Acta, Mol. Cell Biol. Lipids* **2009**, DOI: doi:10.1016/j.bbalip.2009.08.005.
- (27) McGraw, T. E.; Greenfield, L.; Maxfield, F. R. Functional expression of the human transferrin receptor cDNA in Chinese hamster ovary cells deficient in endogenous transferrin receptor. *J. Cell Biol.* **1987**, *105*, 207–214.
- (28) Sun, Y.; Hao, M.; Luo, Y.; Liang, C.; Silver, D. L.; Cheng, C.; Maxfield, F. R.; Tall, A. R. Stearoyl CoA Desaturase Inhibits ATP-binding Cassette Transporter A<sub>1</sub>-mediated Cholesterol Efflux and Modulates Membrane Domain Structure. *J. Biol. Chem.* **2003**, *278*, 5813–5820.
- (29) Wang, Y.; Castoreno, A. B.; Stockinger, W.; Nohrturfft, A. Modulation of Endosomal Cholesteryl Ester Metabolism by Membrane Cholesterol. *J. Biol. Chem.* **2005**, *280*, 11876–11886.
- (30) Brown, M. S.; Goldstein, J. L. The SREBP Pathway: Regulation of Cholesterol Metabolism by Proteolysis of a Membrane-bound Factor. *Cell* **1997**, *89*, 331–340.